Recurrence time distribution in mushroom billiards with parabolic hat

Hiroyuki Tanaka* and Akira Shudo
Department of Physics, Tokyo Metropolitan University, Minami-Ohsawa, Hachioji, Tokyo 192-0397, Japan
(Received 16 June 2006; published 26 September 2006)

The recurrence time distribution of mushroom billiards with a parabolic-shaped hat is investigated. Classical dynamics exhibits sharply divided phase space, and the recurrence time distribution obeys the algebraic law like well-known classes of billiards. However, due to the existence of a specific type of marginally unstable periodic orbits that forms a crossing in phase space, the sticky motion occurs not as a simple drift along the straight line. Numerical experiments reveal and also theoretical analyses predict that an exponent for the cumulative recurrence time distribution approaches 2 in the asymptotic regime, but in a relatively small recurrence time scale it significantly deviates from the predicted universality, which is explained by the slowdown behavior around a crossing point of the periodic orbit family.

DOI: 10.1103/PhysRevE.74.036211 PACS number(s): 05.45.-a

I. INTRODUCTION

Generic Hamiltonian systems are neither completely integrable nor fully chaotic, but rather phase space is typically a mixture of quasiperiodic and chaotic regions. The orbits even in the chaotic regions are strongly influenced by regular components in phase space, and the long-time correlation deviates from that expected in the uniformly hyperbolic situation [1–8]. Highly nontrivial statistical behaviors in mixed phase space originate from complex hierarchical KAM (Kolmogorov-Arnold-Moser) island chains or Cantori, which often appear in the border between regular and chaotic regions.

There are many ways to characterize statistical properties of dynamics. The decay of correlation of dynamical variables or its Fourier transform are well-known measures. Eigenvalues of the Perron-Frobenius operator also provide information on long time decaying characteristics. Among them, because of the statistical reliability in numerical simulations, the recurrence time distribution is very useful and so has attracted much attention. Here the recurrence time t is defined as the first return time after leaving a certain given region, and we consider the distribution of the first return time,

$$P(t)dt = \sharp\{\text{the first return time in } [t, t+dt]\}. \tag{1}$$

The cumulative recurrence time distribution $Q(T)$ is then introduced as

$$Q(T) = \sum_{t=T}^{\infty} P(t) = \lim_{N\to\infty} \frac{N_T}{N}, \tag{2}$$

where N_T is the number of recurrence in a given region with the recurrence time $t > T$ and N denotes the total number of recurrences. Numerical experiments together with theoretical arguments suggest that in systems with hierarchical phase space $Q(T)$ obeys the power law [4,11,12,16–18]

$$Q(T) = T^{-\gamma} \tag{3}$$

with an exponent $\gamma > 1$. Although rigorous analyses verifying it are still lacking, most of the preceding results support the power-law decay and a recent controversial point is the existence of the universal exponent, if any, otherwise to clarify what controls the exponent.

A promising strategy to approach such a problem is, as often done in the study of dynamical systems, to find the simplest possible model that may allow analytical arguments. A class of mushroom billiards invented by Bunimovich certainly fulfills such a requirement [9]. It has mixed phase space in which both chaotic and quasiperiodic regions are coexisting with positive measures. A remarkable fact is that phase space is divided by sharp boundaries with no hierarchical KAM islands, which makes it easy to examine the motion around the boundaries. An analogous type of divided phase space is also realized in the two-dimensional area-preserving map [10]. Concerning the exponent γ, it has been predicted that a family of marginally unstable orbits produces $\gamma = 2$ [11,12]. Since a family of marginally unstable periodic orbits is a main source of power-law behavior of the recurrence time distribution, an argument developed in Refs. [11,12] is applicable to other billiards with so-called bouncing-ball modes [13,14], and thereby $\gamma = 2$ holds also in such a class.

In the present note, as an additional example that provides us with further insights into the issue, we study a deformed version of mushroom billiards, whose precise shape is introduced below, in which a different type of family of marginally unstable periodic orbits emerges as a result of a specific shape of the hat region of the mushroom. We shall demonstrate that the exponent γ for the (cumulative) recurrence time distribution follows the predicted universal behavior only in a very long time regime, and it significantly deviates from it in a relatively short time scale.

II. MUSHROOM BILLIARDS WITH PARABOLIC HAT AND RECURRENCE TIME DISTRIBUTION

Let us first introduce the mushroom billiard with a parabolic boundary. As depicted in Fig. 1(a), the boundary of the

*Present address: Graduate School of Frontier Sciences, University of Tokyo, Chiba 277-5861, Japan.

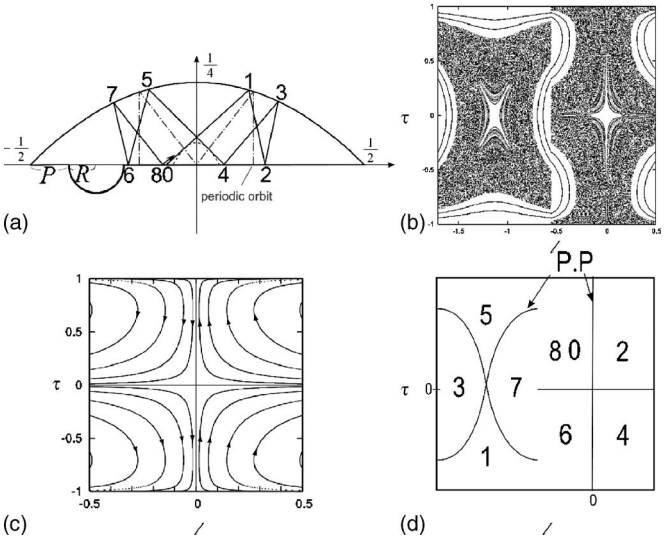

FIG. 1. (a) Mushroom billiard with a parabolic hat. One of marginally unstable periodic orbit forming a one-parameter family is shown as a dark gray line. The numbers inserted represent the regions shown in (d). (b) Phase space in the Birkhoff coordinate with $P=0.2$ and $R=0.05$. (c) The flow lines around the crossing point. (d) A periodic orbit family in phase space (schematic).

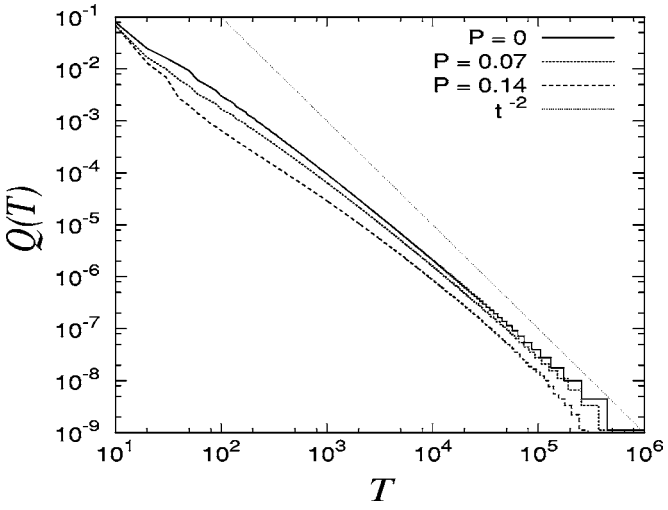

FIG. 2. Cumulative recurrence time distribution for the mushroom billiard with the parabolic with $R=0.15$.

hat region is composed of a parabolic curve and straight segments with a circular-shaped foot. Note that an analogous lemon-shaped billiard with parabolic boundaries generates a typical mixed-type phase space [15]. This is because the focal points of two facing parabolic curves do not coincide in the latter case; otherwise, it is completely integrable. Therefore, it is an important condition that the focal point of the parabola is just on the straight segment. As shown below, the existence of the focal point indeed introduces an interesting structure in phase space.

The dynamics in the billiard table is described by the billiard map F acting on the so-called Birkhof coordinate (ℓ,τ); ℓ denotes the perimeter length along the boundary, and $\tau=\sin\varphi$, where φ is the angle between the reflected direction of the trajectory and the inner normal vector at the bouncing point. Numerical results imply that, as in the case of mushroom billiards with the circular or elliptic hat, regular and chaotic regions are sharply divided, as seen in Fig. 1(b). In addition, a family of marginally unstable periodic orbits, whose period is 8, forms the crossings in phase space. As shown in Fig. 1(d), there are two crossings whose centers correspond to a period-2 periodic orbit that bounces vertically at the center of the hat. Figure 1(c) illustrates the flow lines around a crossing point (0, 0) that is sited in the right part of phase space. In the present setting, if $2R+P<1/2$, that is, if the focal point of the parabola is not contained inside the billiard table, the crossing of marginally unstable families remains.

Taking the foot region as the recurrence region, denoted by $\mathcal{R}$ hereafter, we numerically computed the cumulative recurrence time distribution $Q(T)$ for various P with a fixed R. As demonstrated in Fig. 2, the distributions have algebraic decaying parts as long as the foot does not contain the focal point. We could expect such a power-law behavior since our billiard also has a family of periodic orbits. It should be noted, however, that in a relatively short time scale the exponents deviate from $\gamma=2$, which is conjectured to be universal in the case of stadium or mushroom billiards [11,12,14], and the slopes of the curves in Fig. 2 change gradually in the longer time scale. The result implies that there exists a certain source that leads to the deviation from an expected universality: as mentioned above, the periodic orbit family crosses in phase space and the nature of stickiness differs from that in simpler types of periodic orbits families.

III. THEORETICAL ANALYSIS

A. Expression for one-step drift

In order to understand how the sticky motion occurs under the presence of the crossing point, we first draw the incident and escaping regions for the orbits starting at the recurrence region $\mathcal{R}$. We define the incident and nth escaping regions in each sector as

$$\mathcal{I}=\{(\ell,\tau)|F^{-2}(\ell,\tau)\in\mathcal{R}\} \tag{4}$$

$$\mathcal{E}_n=\{(\ell,\tau)|F^{k}(\ell,\tau)\notin\mathcal{R}(k\leqslant 8(n-1)),$$

$$F^{k}(\ell,\tau)\in\mathcal{R}(8(n-1)<k\leqslant 8n)\}. \tag{5}$$

Here, the factor 8 in the exponent comes from that periodic orbits forming the family is period 8. If $(\ell,\tau)\in\mathcal{I}\cap\mathcal{E}_n$, then the orbit starting at $F^{-2}(\ell,\tau)$ goes out of $\mathcal{R}$ within two steps (it first hits the hat part) and returns back to $\mathcal{R}$ after k iterations, where k is either from $8(n-1)+1$ to $8n$. As a result, we have only to focus on the region around the origin O. Figure 3 illustrates the incident and escaping regions around the origin O. We note that as n becomes large the boundaries of escaping regions accumulate to the lines representing the periodic orbit family. The orbits contained in the region $\mathcal{I}\cap\mathcal{E}_n$ for sufficiently large n stay outside the recurrence region $\mathcal{R}$

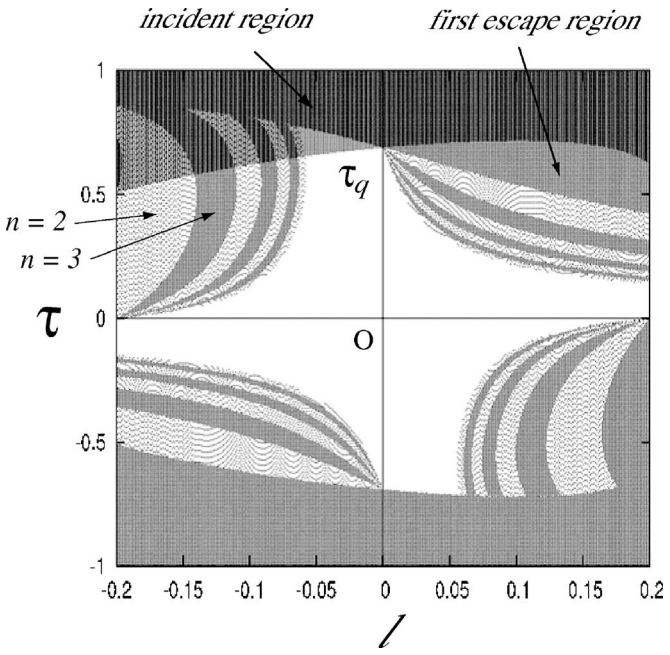

FIG. 3. The incident region $\mathcal{I}$ (upper light gray zone) and the escaping regions $\mathcal{E}_n$. The recurrence region $\mathcal{R}$ is located just outside this figure, i.e. $\ell<-0.2$. The incident region $\mathcal{I}$ and the first escaping region $\mathcal{E}_1$ (upper dark gray zone) crosses at $(0,\tau_q)=F^2(-0.2,0.0)$. The parameters are chosen as $P=0.0$ and $R=0.15$.

for a long time, and thus, they control the long time behavior of recurrent orbits. In phase space, as shown in Fig. 2(c), an orbit put in $\mathcal{I}\cap\mathcal{E}_n$ goes first downward along the periodic orbit family and then turns to the horizontal direction. It moves along the horizontal family and finally returns back to $\mathcal{R}$. In the case of the one-parameter periodic orbit family formed in the stadium or mushroom billiards with a circular hat, the amount of drift along the periodic orbit family per unit step does not depend on the position as long as the orbit moves along it. As mentioned just below, an local argument leads that it is proportional to the distance from the periodic orbit family. In the present case, on the other hand, it does depend on the position of the orbit, which indeed causes different characteristics in the recurrence time statistics.

To be precise, let $(0,\tau_q)$ be the point at which the border of the incident region and $\ell=0$, i.e., the periodic orbit family in the vertical direction, intersects. Suppose an orbit placed on $(-w,\tau_q)$ $(0<w\ll 1)$ and consider the recurrence time $T(w)$ for such an orbit, which is defined via the following relation:

$$\sum_{n=1}^{T(w)} L(n,w) \simeq C(w), \tag{6}$$

where $L(n,w)$ denotes the distance an orbit gains within a single step iteration, and $C(w)$ is the total distance along the curve connecting the point $(-w,\tau_q)$ and the edge of $\mathcal{R}$. As discussed in Ref. [12], in the case of the stadium or mushroom billiards, $L(n,w)$ does not depend on n and is given simply as $L(n,w)=aw$ (a:const) and $C(w)=$const, so that the recurrence time is given as

$$T(w) \sim 1/w \quad (w \ll 1). \tag{7}$$

Thus, the asymptotic distribution of $P(T)$ is expressed as a function of the distribution of perturbations $p(w)$ as

$$P(T(w)) \sim \frac{p(w)}{|dT/dw|} \sim p(w)w^2. \tag{8}$$

Taking into account the recurrence effect [14,16], or an estimate for the overlap between the incident and escaping regions [17], we have $p(w)\sim w$, which leads to $P(T)\sim T^{-3}$ and $Q(T)\sim T^{-2}$. This accounts for the exponent $\gamma=2$ [12].

A key ingredient in the above arguments is, therefore, the amount of drift $L(n,w)$ gained at each n. Since the speed of the orbit slows down as it approaches the crossing point O, we can expect that $L(n,w)$ first decreases as a function of n, then, as the orbit passes in the vicinity of O, $L(n,w)$ again increases.

More detailed evaluation of $L(n,w)$ can be made using the linearized matrices for the periodic orbit family. The linearized matrices for vertical and horizontal directions are given, respectively, as

$$DF^8(\ell,0) = \begin{pmatrix} 1 & -8\ell^2 \\ 0 & 1 \end{pmatrix} \quad -\frac{1}{2} < \ell < \frac{1}{2}, \tag{9}$$

$$DF^8(0,\tau) = \begin{pmatrix} 1 & 0 \\ 8\tau^2(1-\tau^2) & 1 \end{pmatrix} \quad -1 < \tau < 1. \tag{10}$$

The flow lines along which the orbit moves are parametrized by α

$$\ell = -\frac{\alpha}{\tau\sqrt{1-\tau^2}}, \tag{11}$$

where $\alpha=w\tau_q\sqrt{1-\tau_q^2}$. On the configuration space, the set of lines whose envelope function is given as a parabola $y=\ell^2/4\alpha+\alpha$ intersect with the straight segment of the hat at (ℓ,τ).

Now, we derive $L(n,w)$ for the process along the vertical and horizontal lines, denoted by $L_{\mathrm{ver}}(n,w)$, $L_{\mathrm{hor}}(n,w)$, respectively. An orbit starting at $(-w,\tau_q)$ shifts downward along the vertical line $\ell=0$. The linearized matrix (10), together with the relation (11), gives a linearized map on the curve (11) as

$$\ell = -\frac{\alpha}{\tau\sqrt{1-\tau^2}}, \tag{12}$$

$$\tau' = 8\tau^2(1-\tau^2)\ell + \tau. \tag{13}$$

Thus, under the condition $\ell\ll 1$, the recursion relation for τ is approximated by a differential equation,

$$\frac{d\tau}{dt} = -8\alpha\tau\sqrt{1-\tau^2}. \tag{14}$$

The solution for the initial condition $\tau(0)=\tau_q$ is

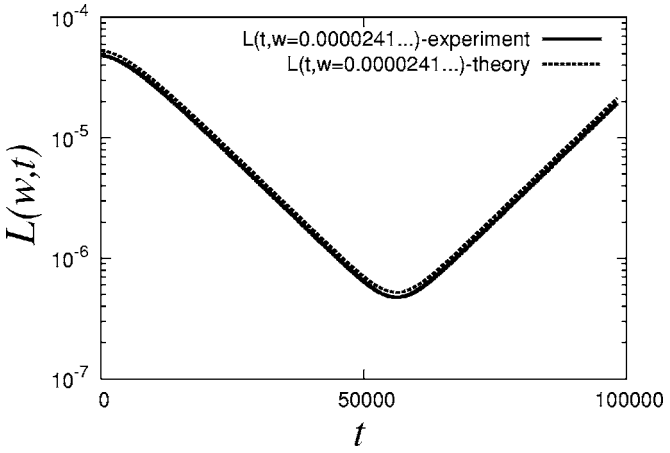

FIG. 4. $L(n,w)$ for $w=0.00002\,41885\,52601\,9499\ldots$.

$$\tau(t)=\frac{2\sqrt{\delta e^{-16\alpha t}}}{1+\delta e^{-16\alpha t}},\quad \text{where}\quad \delta=\frac{1-\sqrt{1-\tau_q^2}}{1+\sqrt{1-\tau_q^2}}. \tag{15}$$

Hence,

$$L(w,t)\simeq L_{\mathrm{ver}}(w,t)=16\alpha\sqrt{\delta}e^{-8\alpha t}\frac{1-\delta e^{-16\alpha t}}{(1+\delta e^{-16\alpha t})^2}. \tag{16}$$

Similarly, we give $L_{\mathrm{hor}}(n,w)$ for the process along the horizontal line. Under the condition $\tau\ll 1$, we approximate the right-hand side of the relation (11) as $\ell\simeq-\alpha/\tau$ $(\alpha>0)$ to give the recursion relation for ℓ

$$\ell'=\ell+8\alpha\ell. \tag{17}$$

Note that $\ell(t=T)=\ell_r$ where ℓ_r denotes the ℓ coordinate of the recurrence region $\mathcal{R}$. Then, we have

$$L(w,t)\simeq L_{\mathrm{hor}}(w,t)=8\alpha\ell_r e^{8\alpha(t-T)}. \tag{18}$$

Finally, we evaluate $L(n,w)$ in the vicinity of the crossing point O. If an orbit is passing around the crossing point O, we have to take into account the influence either from the vertical and horizontal family. Since the recursion relations for τ and ℓ derived above are compatible via the relation (11), the leading-order contribution from $L_{\mathrm{ver}}(w,t)$ and $L_{\mathrm{hor}}(w,t)$ should be incorporated as

$$L(w,t)\simeq\sqrt{L_{\mathrm{ver}}(w,t)^2+L_{\mathrm{hor}}(w,t)^2}. \tag{19}$$

Indeed, as shown in Fig. 4, $L(w,t)$ thus derived well reproduces a curve that is numerically obtained.

Combining these three processes, we have an integral expression for (6)

$$C(w)\simeq\int_0^T L(w,t)dt \tag{20}$$

$$\simeq\int_0^{\alpha T}8e^{8s}\sqrt{4\delta\frac{(e^{16s}-\delta)^2}{(e^{16s}+\delta)^4}+\ell_r^2e^{-16\alpha T}}ds. \tag{21}$$

Since the right-hand side is a function of αT and $C(w)\to\ell_r+\tau_q$ as $w\to 0$, which means $C(w)$ is constant, αT is constant. Recall that α is written as $\alpha=w\tau_q\sqrt{1-\tau_q^2}$; thus, we have $T\propto 1/w$. Hence, in the asymptotic limit, we expect that the scaling exponent $\gamma=2$, which is the same as the stadium or mushroom billiards with a circular hat. However, the way of convergence is more subtle.

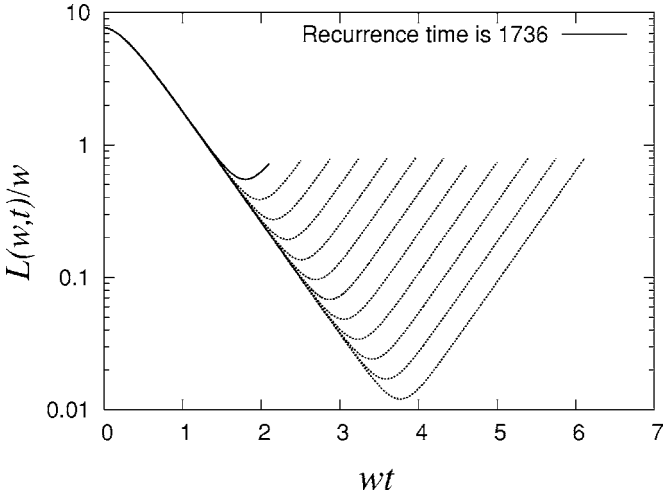

FIG. 5. Logarithmic plot of $L(t)/w$ as a function of wt. The left-most curve (solid curve) is the case with the recurrence time 1736 and $w=0.00125$, and w in each curve is reduced to half, one after another.

B. Asymptotic behavior of recurrence time

In order to see $L(w,t)$ in the limit of $w\to 0$ more closely, we plotted in Fig. 5 $L(w,t)/w$ as a function of wt. Note that $L(w,t)/w$ is constant in the case of simple periodic orbit families appearing stadium or Sinai billiards. We can see that the regions in each curve, which correspond to the parallel drift along the vertical and horizontal family, respectively, obey the same scaling functions. This is because the linear relation between $L(w)$ and w holds during those processes. In the vicinity of O, however, the linear relation is broken and the degree of stickiness becomes larger as w is reduced. This is the reason why the curves $L(w,t)/w$ are prolonged.

Furthermore, we note from Fig. 5 that the amount of prolongation is constant as w is reduced to rw $(0<r<1)$. This leads a relation

$$rwT(rw)-wT(w)=-c\ln r\quad (c>0:\text{const}). \tag{22}$$

Putting $f(w)=wT(w)$ and $r=1+\varepsilon$ $(\varepsilon<0)$, we have

$$\lim_{h\to 0}\frac{f(w+h)-f(w)}{h}=\lim_{h\to 0}(-c)\ln\left[\left(1+\frac{h}{w}\right)^{1/h}\right], \tag{23}$$

where $h=\varepsilon w$. Thus, we obtain a differential equation for $f(w)$

$$\frac{df(w)}{dw}=-\frac{c}{w}, \tag{24}$$

and the recurrence time $T(w)$ is expressed as

$$T(w)=\frac{-c\ln w+d}{w}\quad (d:\text{const}). \tag{25}$$

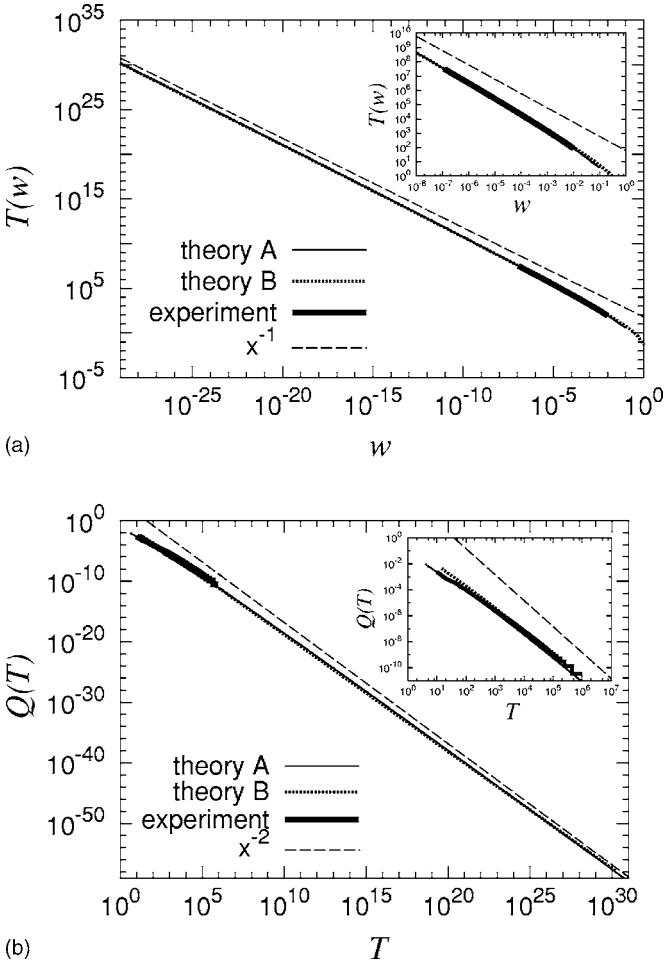

FIG. 6. (a) The recurrence time $T(w)$ and (b) the cumulative recurrence time distribution $Q(T)$ for numerical experiments, the theoretical result using the expression (20) (theory A), and that assuming the behavior (22) (theory B). A set of parameters is the same as those used in Fig. 4.

Recall that $T(w)=1/w$ holds in the case of the simple periodic orbit family. This logarithmic correction exactly reflects the slowdown process in the vicinity of O, and therefore, the deviation from $\gamma=2$ in relatively small T in the cumulative recurrence time distribution originates from it.

As shown in Fig. 6, theoretical results obtained by a direct calculation using (20) and also obtained by assuming the relation (22) are compared to a numerical result. Both theoretical predictions reproduce well the numerical curve, and for an exceedingly large recurrence time regime, which is far beyond the numerical experiments, it is shown that the exponent γ indeed tends to 2 as predicted above.

IV. CONCLUDING REMARKS

We have studied the recurrence time distribution for mushroom billiards with parabolic hat. Because of the presence of a focal point of the parabola, the periodic orbit family forms a crossing in phase space, not a simple straight line. Such a specific structure in phase space certainly causes anomalously slow dynamics, which is different from the one with simple periodic orbit families.

Asymptotically, it is predicted that the distribution function obeys the power law with its exponent $\gamma=2$, which is the same as the exponent derived for the system with simple periodic orbit family or sharply divided phase space. However, in a relatively small recurrence time regime, it was found numerically the deviation from the $\gamma=2$ is significant. The theoretical analysis was done so that the deviation numerically observed certainly has an origin that is related to the slowdown process around the crossing point of the periodic orbit family. Under a certain assumption, we obtained an expression of the recurrence time $T(w)$ as a function of w. The logarithmic correction thus derived explains the deviation in the small recurrence time regime.

[1] C. F. F. Karney, Physica D **8**, 360 (1983).
[2] B. V. Chirikov and D. L. Shepelyansky, Physica D **13**, 395 (1984).
[3] G. M. Zaslavsky, Phys. Rep. **371**, 461 (1984).
[4] F. Vivaldi, G. Casati, and I. Guarneri, Phys. Rev. Lett. **51**, 727 (1983).
[5] J. D. Meiss and E. Ott, Phys. Rev. Lett. **55**, 2741 (1985); Physica D **20**, 387 (1986).
[6] R. S. Mackay, J. D. Meiss, and I. C. Percical, Physica D **13**, 55 (1984).
[7] T. Geisel, A. Zacherl, and G. Radons, Phys. Rev. Lett. **59**, 2503 (1987).
[8] Y. Aizawa, Y. Kikuchi, T. Harayama, K. Yamamot, M. Ota, and K. Tanaka, Prog. Theor. Phys. Suppl. **98**, 36 (1989).
[9] L. A. Bunimovich, Chaos **11**, 802 (2001); **13**, 903 (2003).
[10] J. Malovrh and T. Prosen, J. Phys. A **35**, 2483 (2002).
[11] E. G. Altmann, A. E. Motter, and H. Kantz, Chaos **15**, 033105 (2005).
[12] E. G. Altmann, A. E. Motter, and H. Kantz, Phys. Rev. E **73**, 026207 (2006).
[13] P. Gaspard and J. R. Dorfman, Phys. Rev. E **52**, 3525 (1995).
[14] D. N. Armstead, B. R. Hunt, and E. Ott, Physica D **193**, 94 (2004).
[15] V. Lopac, I. Mrkonjić, and D. Radić, Phys. Rev. E **59**, 303 (1999).
[16] B. V. Chirikov and D. L. Shepelyansky, Phys. Rev. Lett. **82**, 528 (1999).
[17] T. Miyaguchi, Ph.D thesis, Waseda University, 2006 (unpublished) (in Japanese).
[18] M. Weiss, L. Hufnagel, and R. Ketzmerick, Phys. Rev. E **67**, 046209 (2003); Phys. Rev. Lett. **89**, 239401 (2002).